Physics-informed neural networks for 1D sound field predictions with parameterized sources and impedance boundaries

Nikolas Borrel-Jensen[1], Allan P. Engsig-Karup[2], Cheol-Ho Jeong[1]

[1] Acoustic Technology, Dep. of Electrical Engineering, Technical University of Denmark, 2800 Kgs. Lyngby, DK
[2] Dep. of Applied Mathematics and Computer Science, Technical University of Denmark, 2800 Kgs. Lyngby, DK

Realistic sound is essential in virtual environments, such as computer games and mixed reality. Efficient and accurate numerical methods for pre-calculating acoustics have been developed over the last decade; however, pre-calculating acoustics makes handling dynamic scenes with moving sources challenging, requiring intractable memory storage. A physics-informed neural network (PINN) method in 1D is presented, which learns a compact and efficient surrogate model with parameterized moving Gaussian sources and impedance boundaries, and satisfies a system of coupled equations. The model shows relative mean errors below 2%/0.2 dB and proposes a first step in developing PINNs for realistic 3D scenes.

The Wave Equation

The wave equation is describing how sound waves propagate

$$\frac{\partial^2 p(x,t)}{\partial t^2} - c^2 \frac{\partial^2 p(x,t)}{\partial x^2} = 0, \qquad t \in \mathbb{R}^+, \qquad x \in \Omega.$$

where p is the pressure (Pa), t is the time (s) and c is the speed of sound in air (m/s). The initial conditions (ICs) are satisfied by using a Gaussian source for the pressure part and setting the velocity equal to zero

$$p(x, t=0, x_0) = \exp\left[-\left(\frac{x - x_0}{\sigma_0}\right)^2\right], \qquad \frac{\partial p(x, t=0, x_0)}{\partial t} = 0,$$

with σ_0 being the width of the pulse determining the frequencies to span.

Frequency-independent BCs are given by

$$\frac{\partial p}{\partial t} = -c\xi \frac{\partial p}{\partial \mathbf{n}},$$

where $\xi = Z_s/(\rho_0 c)$ is the normalized surface impedance, ρ_0 denotes the air density (kg/m^3) and Z_s is the impedance.

Frequency-dependent BCs are given by

$$v_n(t) = Y_\infty p(t) + \sum_{k=0}^{Q-1} A_k \phi_k(t) + \sum_{k=0}^{S-1} 2\left[B_k \psi_k^{(0)}(t) + C_k \psi_k^{(1)}(t)\right],$$

$v_n(t)$ being the velocity at a boundary and the accumulators ϕ_k , $\psi_k^{(0)}$ and $\psi_k^{(1)}$ determined by solving the coupled ADEs

$$\frac{d\phi_k}{dt} + \lambda_k \phi_k = p, \qquad \frac{d\psi_k^{(0)}}{dt} + \alpha_k \psi_k^{(0)} + \beta_k \psi_k^{(1)} = p, \qquad \frac{d\psi_k^{(1)}}{dt} + \alpha_k \psi_k^{(1)} - \beta_k \psi_k^{(0)} = 0,$$

where Q is the number of real poles λ_k, S is the number of complex conjugate pole pairs $\alpha_k \pm j\beta_k$, and Y_∞, A_k, B_k and C_k are numerical coefficients determined using e.g. Miki's model for a porous material.

The boundary conditions are formulated by inserting the calculated velocity v_n into the pressure term of the linear coupled wave equation $\frac{\partial p}{\partial \mathbf{n}} = -\rho_0 \frac{\partial v_n}{\partial t}$.

Physics-informed Neural Networks

Two multi-layer feed-forward neural networks are setup as depicted in Fig. 1

$$\hat{f} : (x, t, x_0) \mapsto \mathcal{N}_f(x, t, x_0; \mathbf{W}, \mathbf{b}), \qquad \hat{g} : (x, t, x_0) \mapsto \mathcal{N}_{\text{ADE}}(x, t, x_0; \mathbf{W}, \mathbf{b}),$$

where $\mathbf{W}$ and $\mathbf{b}$ are the network weights and biases, respectively; x is the receiver position, t is the time, and x_0 is the source position. $\mathcal{N}_{ADE}$ is only for freq.-dep. BCs.

NOTE: In contrary to "black box" deep learning, the underlying physics are included in the training and their residual minimized through the loss function in PINNs.

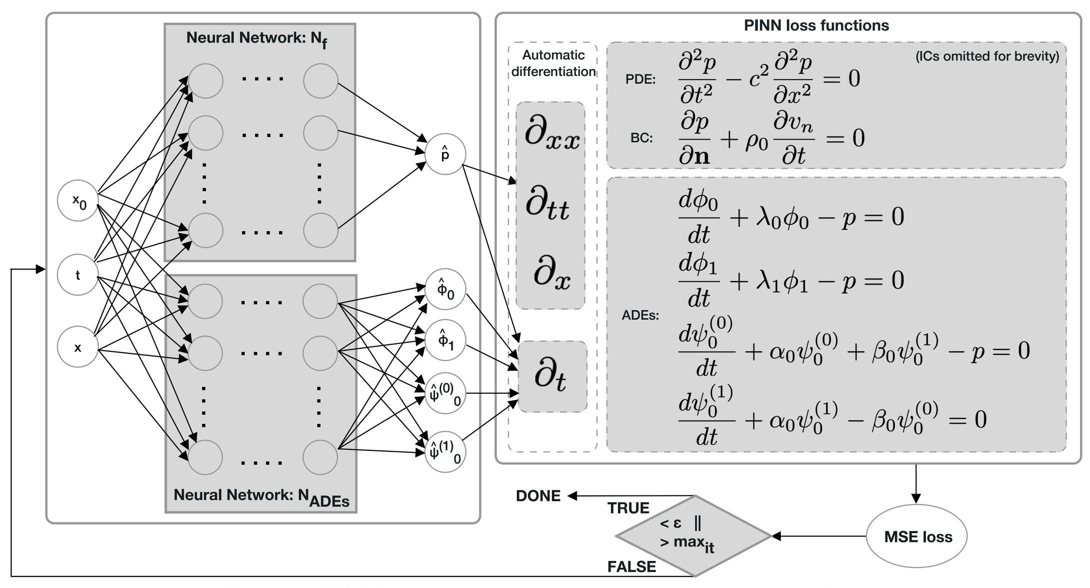

Figure 1. PINN scheme for frequency-dependent boundaries.

The freq.-indep. minimisation problem is

$$\arg\min_{\mathbf{W},\mathbf{b}} \mathcal{L}(\mathbf{W}, \mathbf{b}) = \mathcal{L}_{\text{PDE}} + \lambda_{\text{IC}}\mathcal{L}_{\text{IC}} + \lambda_{\text{BC}}\mathcal{L}_{\text{BC}}$$

where

$$\mathcal{L}_{\text{PDE}} = \|\frac{\partial^2}{\partial t^2}\mathcal{N}_f(x_f^i, t_f^i, x_{0,f}^i; \mathbf{W}, \mathbf{b}) - c^2\nabla^2\mathcal{N}_f(x_f^i, t_f^i, x_{0,f}^i; \mathbf{W}, \mathbf{b})\|,$$

$$\mathcal{L}_{\text{IC}} = \|\mathcal{N}_f(x_{\text{IC}}^i, 0, x_{0,ic}^i; \mathbf{W}, \mathbf{b}) - \exp\left[-\left(\frac{x - x_0}{\sigma_0}\right)^2\right]\| + \|\frac{\partial}{\partial t}\mathcal{N}_f(x_{\text{IC}}^i, 0, x_{0,ic}^i; \mathbf{W}, \mathbf{b})\|,$$

$$\mathcal{L}_{\text{BC}} = \|\frac{\partial}{\partial t}\mathcal{N}_f(x_{\text{BC}}^i, t_{\text{BC}}^i, x_{0,bc}^i; \mathbf{W}, \mathbf{b}) + c\xi\frac{\partial}{\partial \mathbf{n}}\mathcal{N}_f(x_{\text{BC}}^i, t_{\text{BC}}^i, x_{0,bc}^i; \mathbf{W}, \mathbf{b})\|$$

For freq.-dep. BCs the loss $\mathcal{L}_{\text{ADE}}$ should be added to minimisation problem.

Results and Conclusion

Freq.-indep. (Fig. 2) and dep. (Fig. 3) BCs are tested, each with parameterized moving sources trained at seven evenly distributed positions $\mathbf{x}_0 = [-0.3, -0.2, \ldots, 0.3]$ m and evaluated at $\mathbf{x}_0 = [-0.3, -0.15, 0.0, 0.15, 0.3]$ m.

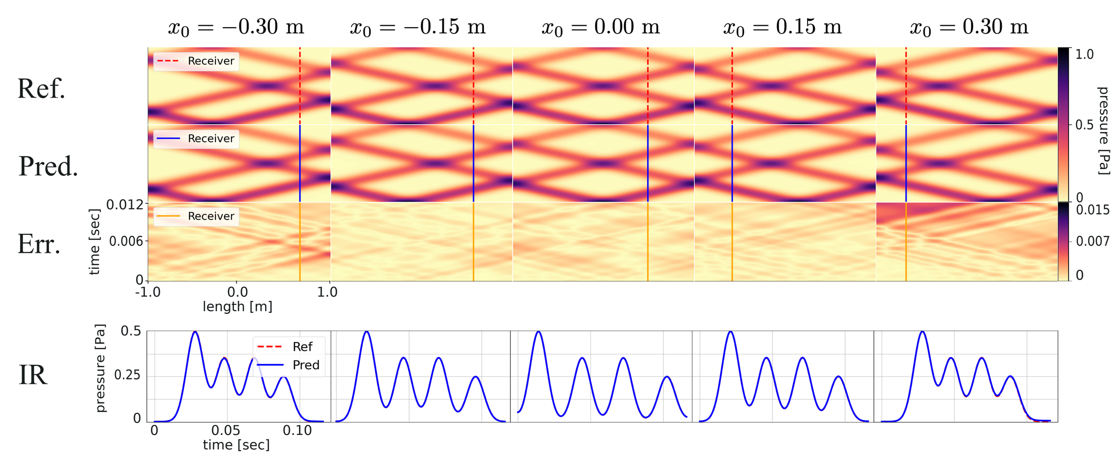

Figure 2. Frequency-independent impedance boundaries evaluated at five source positions.

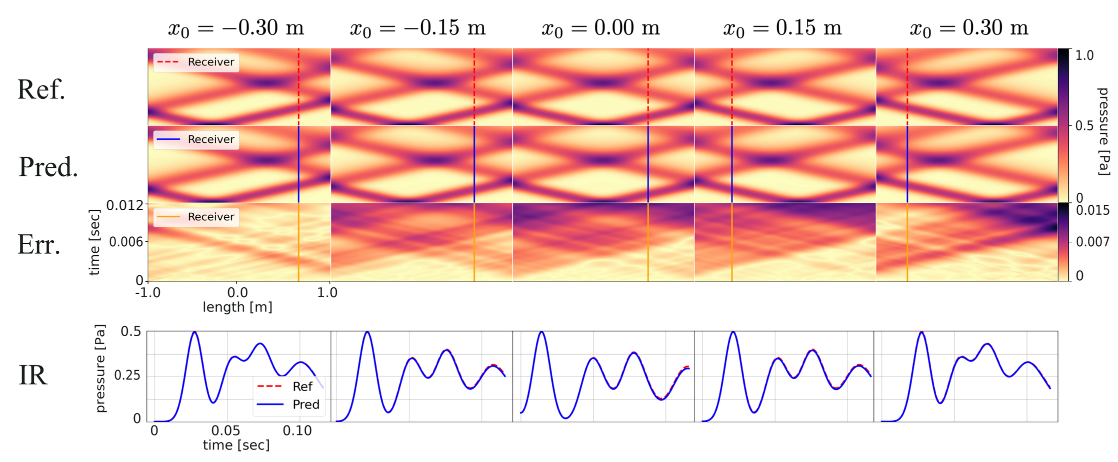

Figure 3. Frequency-dependent impedance boundaries evaluated at five source positions.

The relative errors $\mu_{rel}(x, x_0)$ are all below 2% indicating good predictions with no perpetual differences.

Nikolas Borrel-Jensen <nibor@elektro.dtu.dk>